EARTHQUAKE ENGINEERING AND STRUCTURAL DYNAMICS, VOL. 25, 1373–1389 (1996)

SEISMIC IMPACT LOADING IN INELASTIC TENSION-ONLY CONCENTRICALLY BRACED STEEL FRAMES: MYTH OR REALITY?

ROBERT TREMBLAY* AND ANDRÉ FILIATRAULT†

Department of Civil Engineering, Ecole Polytechnique, University of Montreal Campus, P.O. Box 6079, Station "Centre-Ville", Montreal, Canada H3C 3A7

SUMMARY

Tension-Only Concentrically Braced Frames (TOCBF) exhibit deteriorating pinched hysteretic behaviour during strong earthquakes. Slender braces transit between an elastic buckling state, a restraightening state, in which they carry almost no load, an elastic tensile loading state as they are suddenly taut and, finally, a tensile yielding state. It has long been suspected that the sudden increase in tensile forces in the braces of TOCBSF creates detrimental impact loading on the connections and other structural elements. No experimental evidence, however, has been provided so far to confirm, or to quantify, this impact phenomenon. This paper addresses this issue through shake table tests of half scale, two-storey, TOCBF models. By normalizing the hysteresis loops of braces obtained from shake table tests to the yield strength of steel obtained from quasi-static tests, the increase in tensile forces in the braces was obtained. Results of dynamic tensile tests on steel coupons under similar strain rates as observed during the shake table tests showed that this increase in tensile forces is not the result of impact, but is rather caused by a yield strength increase of the steel under high strain rate. A procedure is proposed to estimate and account for this increase in tensile forces in the braces at the design stage.

KEY WORDS: braced frames; impact; seismic; shake table; strain rates; steel

INTRODUCTION

Concentrically Braced Frames (CBF), for which the bracing elements intersect the centre lines of the joint members, have long been recognized as a practical and efficient way to resist lateral forces.[1] CBF resist lateral inertia forces from a strong earthquake by a vertical truss mechanism consisting of alternating tension and compression forces in the bracing members. CBF can be classified into two categories depending on the ability of the braces to sustain compression loads before buckling.

The bracing elements of the first category, known as 'tension–compression' CBF, exhibit sufficient compression strength to dissipate a significant amount of energy through inelastic buckling. This system, capable of providing a stable ductile behaviour under severe lateral cyclic loading, has been favoured by building codes based on several analytical and experimental investigations.[2–11]

The second category, known as Tension-Only Concentrically Braced Frames (TOCBF), incorporates very slender bracing members (such as steel rods or flat plates) which are unable to dissipate much energy in compression. A characteristic of TOCBF is their deteriorating pinched hysteretic behaviour during strong earthquakes. Alternating tension yielding and compression buckling of the bracing elements induce slackness in the lateral load resisting system around its point of zero displacement. This slackness translates into severely pinched hysteresis loops and potential impact loading in the structure. This unfavourable behaviour was quickly recognized as a major fault of TOCBF and, therefore, structural engineers have shied away from this system for medium- and high-rise buildings located in active seismic areas.

* Assistant Professor
† Associate Professor

CCC 0098–8847/96/121373–17

Received 13 February 1996
Revised 4 June 1996

TOCBF systems, however, continue to be used extensively for low-rise industrial and commercial steel buildings, particularly in areas of moderate seismicity. These structures constitute a large portion of the building stock in North America. This extensive use of TOCBF, however, has not been accompanied by an adequate research effort to understand fully their behaviour and rationalize their design.

Slender braces in TOCBF transit between an elastic buckling state, a restraightening state, in which they carry almost no load, an elastic tensile loading state as they are suddenly straightened and, finally, a tensile yielding state. North American seismic provisions associate the sudden increase in tensile forces in the braces with detrimental impact loading on the connections and other structural elements.[12–15] The latest edition of NEHRP seismic regulations in the United States recommend to pretension diagonal members in TOCBF to prevent loose diagonals during strong earthquakes.[12] In California, designers are warned that the force demand on a brace in tension is expected to exceed the brace tensile yield strength.[13] The latest edition of the Canadian steel standard[15] specifies an explicit value of 1·10 for an impact factor to be used in the design of the brace connections. No experimental evidence, however, has been provided so far to confirm, or to quantify, this impact phenomenon.

The main objective of this paper is to shed some light on the behaviour of TOCBF through shake table tests of half-scale, two-storey, TOCBF models. The bracing elements were instrumented to measure their hysteretic loops under seismic conditions. By comparing these hysteresis loops with quasi-static and dynamic monotonic test results, the increase in tensile forces in the braces was quantified.

SEISMIC IMPACT LOADING AND STRAIN RATE EFFECT IN TOCBF

Impact loading occurs when a moving body strikes a structure. Based on the principle of conservation of energy, at the instant the moving body is stopped, its kinetic energy is transformed into internal strain energy in the structure. At this instant, vibrations of the structure begin. These vibrations amplify the static response of the structure. This amplification can be accounted for by an impact factor.

The sudden increase in tensile forces in the braces of TOCBF has long been suspected to cause detrimental impact loading on the connections and other structural components of the lateral load resisting system. In fact, two mechanisms can contribute to amplify the forces in the braces during tensile loading.

The first mechanism is a true impact phenomenon caused by a transfer of energy from the floor masses, being suddenly restrained in their motion, to the braces becoming suddenly taut. If the velocity of the floor masses is sufficient, vibrations of the structure can cause an amplification of its response.

The second mechanism is associated with the strain rate effect on the yield strength of the steel. During elastic tensile loading, the braces are subjected to a high strain rate demand. Past investigations regarding the behaviour of steel members under earthquake-type strain rates (less than 10^{-1}/s) mainly originate from Japan[16–20] and the United States.[21] Although the results from the various investigations present a large scatter, similar tendencies have been reported by all researchers. The yield strength of steel increases with the rate of loading while the tensile strength remains almost the same. In addition, the strain rate has a negligible effect on the elastic and strain-hardening moduli of steel. Therefore, if a sufficient tensile strain rate is induced in the braces of TOCBF during a strong earthquake, a portion of the increase in tensile forces in the braces may be attributed to the increase of the yield strength of the steel.

The experimental investigation conducted by Wakabayashi *et al.*[16] is the most applicable to TOCBF under seismic conditions. Dynamic and quasi-static tests of round steel bars under cyclic axial loading were conducted to examine the strain rate effect on the uniaxial stress–strain curves of common mild steel. From these results, the following expression was proposed to estimate the increase of yield strength of steel with strain rate:

$$\frac{F_{yd}}{F_{ys}} = 1 + 0{\cdot}0473 \log\left(\frac{\dot{\varepsilon}}{\dot{\varepsilon}_0}\right) \tag{1}$$

where F_{yd} is the dynamic yield strength for a strain rate $\dot{\varepsilon}$ and F_{ys} is the quasi-static yield strength under a strain rate $\dot{\varepsilon}_0 = 50 \times 10^{-6}$/s.

The shake table, quasi-static, and dynamic monotonic tensile tests conducted in this investigation were aimed at uncoupling the two mechanisms which contribute to the increase in tensile forces in braces of TOCBF. By normalizing the hysteresis loops of the braces as obtained from shake table tests to the static yield strength of steel obtained from quasi-static tensile tests, F_{ys}, the increase in tensile forces in the braces resulting from a combination of the two mechanisms could be obtained. From the results of monotonic tensile tests on steel coupons under similar strain rates as observed during the shake table tests, it was possible to evaluate the contribution of the strain rate effect to the increase in brace tensile forces. The difference between the two results above could therefore be attributed to a pure impact mechanism.

SHAKE TABLE TEST PROGRAM

Description of test frame

Half-scale, two-storey, TOCBF models were tested on the uniaxial, 3·4 m × 3·4 m earthquake simulation facility at Ecole Polytechnique in Montreal, Canada.[22] A general view of the test frame is presented in Figure 1. The two-storey plane frame has a total height of 3·6 m. The two continuous columns were made of a W250 × 58 steel sections.

To represent a simply supported base, each base column was linked to a true pin mechanism which, in turn, was attached to a foundation beam on the shake table. The two pin-ended floor beams were made of Hollow Structural Steel (HSS) 127 × 76 × 4·8 sections.

The mass of the model was simulated by four concrete blocks (30 kN each) linked to the floor beams. These concrete blocks were supported vertically by a peripheral frame. This structure supported all the vertical loads from the concrete blocks so the test frame could carry only the lateral inertia loads. This peripheral frame was completely pinned in the direction of the shake table motion and braced in the opposite direction

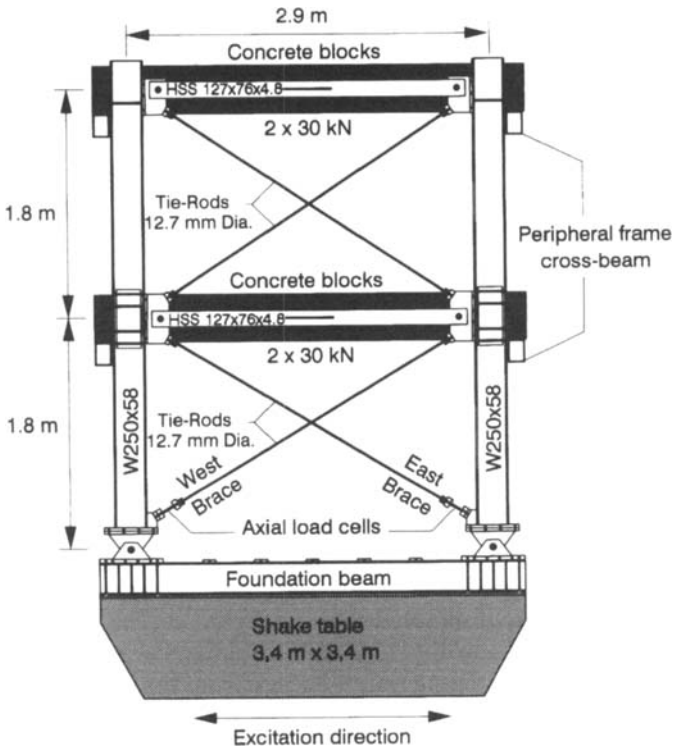

Figure 1. Test structure

Figure 2. Test and supporting structures after a seismic test on shake table

to ensure no motion of the test plane frame in that direction. Figure 2 shows a photograph of the test frame and supporting structure after a seismic test on the shake table.

In the direction of excitation, the test frame was braced at each level by grade 300 W steel round tie-rods having a diameter of 12·7 mm. These braces were very slender with a slenderness ratio of 800 and exhibited negligible buckling strength. Two axial load cells were placed adjacent to the bottom first floor brace connections as shown in Figure 3. The force time-histories of both first floor braces could be recorded with these load cells. The second floor braces were not instrumented. Three different seismic tests were carried out, involving six different first floor braces. Table I presents the yield and tensile strength obtained from quasi-static ($\dot{\varepsilon} = 50 \times 10^{-6}$/s) monotonic tensile tests performed on 150 mm long specimens of each brace material.

Preliminary system identification tests

The dynamic characteristics of the model frame were estimated from low-amplitude ambient vibration simulations and from free vibration tests. For the ambient vibration simulations, the test frame was excited by a 0–25 Hz flat white noise, with an RMS (Root Mean Square) amplitude of 0·03 g. This base motion was large enough to cause buckling in all compression braces at each cycle, but was sufficiently low to ensure that the tension braces remained in the elastic range of the steel. A dedicated ambient vibration analysis software[23] was then used to determine the natural periods of the test frame from power spectral density plots of the absolute floor horizontal acceleration records. In the free vibration tests, the structure was excited by a sinusoidal input at its first natural period. When a steady-state response was obtained, the input was suddenly stopped and the floor relative displacements were recorded. The first modal damping ratio of the structure was then established by the logarithmic relative displacement decrement at each floor.[24]

The natural periods and first modal damping ratio obtained from the preliminary tests are summarized in Table II. The first mode of vibration, at a period of 0·47 s, is a classical shear mode involving tensile and buckling deformations of the braces. The second mode of vibration, at a period of 0·073 s, represents a flexural mode of deformation of the columns.

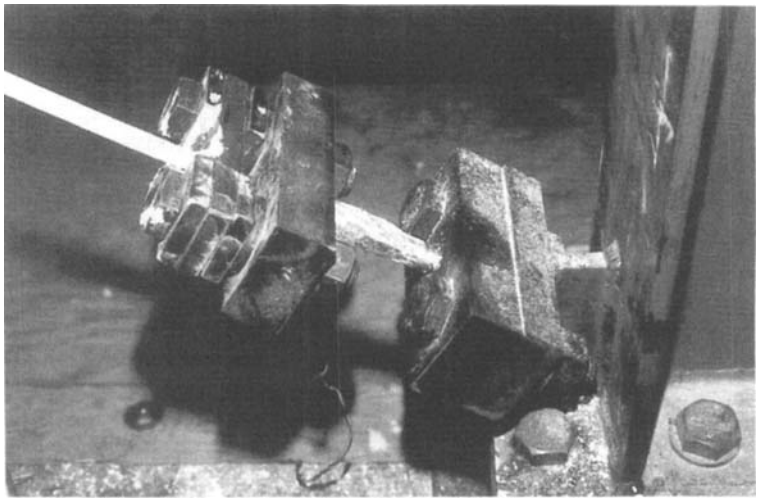

Figure 3. Axial load cell to record force time-history of first floor brace

Table I. Quasi-static yield and tensile strengths of first floor braces

Brace no.	Yield strength F_{ys} (MPa)	Tensile strength F_{us} (MPa)
1	313	474
2	313	473
3	327	475
4	316	463
5	313	459
6	320	467
Mean	317	469

Table II. Experimental natural periods and first modal damping ratio

Natural period* (s)		First modal damping ratio (%)
First mode	Second mode	
0·471 ± 0·005	0·073 + 0·005	2·4

* *Parameters of ambient vibration tests*
Base input: 0–25 Hz flat white noise with RMS amplitude of 0·03 g
Recording increment: 0·02 s
Recording duration: 328 s
Frequency resolution: ± 0·0244 Hz
Number of averaging windows: 8
Number of data points per averaging window: 16 384

SHAKE TABLE TEST RESULTS

Selection and scaling of earthquake ground motions

Three different historical ground motions, recorded in Western North America, were chosen as input for the shake table studies. The characteristics of these records are summarized in Table III. These records

Table III. Historical seismic events considered for shake table tests

Record name	Earthquake name	Station	Date	Component	PHA (g)	PHV (m/s)
Puget Sound	Western Washington	Olympia highway testing laboratory	13-04-49	NO4W	0·16	0·21
San Fernando	San Fernando	Hollywood storage P.E. lot Los Angeles	9-02-71	N90E	0·21	0·21
El Centro	Imperial Valley	El Centro site Imperial Valley Irrigation District	18-05-40	S00E	0·34	0·33

present ratios of Peak Horizontal Acceleration (PHA in g) to Peak Horizontal Velocity (PHV in m/s) close to unity which is compatible with seismic zoning maps of Western Canada.[25]

Each accelerogram was scaled to mobilize a displacement ductility level representative of code designed structures. This scaling procedure was based on equating, for each accelerogram, the base shear at first yield specified in the 1995 edition of the National Building code of Canada (NBCC)[25] to the actual yield base shear of the structure. According to NBCC, the base shear at first yield that a structure is expected to develop, V_{yc}, is given by

$$V_{yc} = \frac{V_e U}{\phi R} \tag{2}$$

where V_e is the base shear that the structure would develop if it would remain elastic, U is a calibration factor equal to 0·6, R is a force reduction factor equal to 2·0 for TOCBF and ϕ is a resistance factor equal to 0·9 for steel.

A two-dimensional linear analysis of the structure was performed for each earthquake accelerogram. The actual yield base shear of the structure, V_{ya}, was calculated by multiplying the elastic base shear obtained from the analysis, $V_{eE/Q}$, by the ratio of the yield tensile load of the braces to the maximum brace force obtained from the analysis. If V_{ya} is to be equal to V_{yc} the accelerogram must be multiplied by a scaling factor SF such that

$$\mathrm{SF}\left(\frac{V_{eE/Q} U}{\phi R}\right) = V_{ya} \tag{3}$$

or

$$\mathrm{SF} = \frac{V_{ya}\phi R}{V_{eE/Q} U} \tag{4}$$

This procedure yielded SF values of 1·3, 1·6 and 1·2 for the Puget Sound, San Fernando and El Centro accelerograms, respectively. Figure 4 presents the absolute acceleration response spectra of the three scaled seismic events for 2·4 percent damping (corresponding to the first modal damping ratio of the structure).

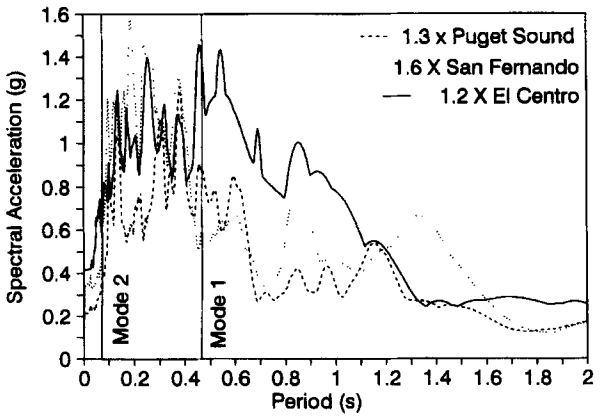

Figure 4. Absolute acceleration response spectra (2·4 per cent damping) for the three scaled accelerograms

Hysteretic behaviour of first floor braces

For each earthquake excitation, the load cells recorded the force time-histories of the first floor braces. Linear potentiometers recorded the absolute lateral displacement time-histories of the shake table and of the first floor mass. By subtracting these two signals and considering the inclination of the braces, the strain time-history of the first floor braces was obtained. By combining the stress and strain time-histories, the stress–strain hysteresis loops in the first floor braces could be drawn.

Figure 5 presents, for the three seismic events considered, the stress–strain hysteresis loops for the first floor brace located on the east side of the frame (see Figure 1). The stress was normalized to the pseudo-static yield strength of each brace, F_{ys}, as given in Table 1. The behaviour of the brace is consistent for the three earthquake records. The brace yields in tension at a strain of about 0·2 per cent and exhibits ductility ratios ranging from 2·4 (for Puget Sound) to 7·7 (for El Centro). The maximum stress recorded in the brace exceeds the pseudo-static yield strength by an identical value of 14 per cent for the three seismic events. This peak value occurs when the brace is stretched significantly, for the first time, in the inelastic range. During the tensile loading state before the first yield excursion, the structure vibrated elastically which caused a maximum strain rate demand in the tension braces. Following the maximum stress, the stress reduces slightly as the brace elongates in the inelastic range. This stress reduction is the result of an increase in the effective period of vibration which reduces the strain rate demand on the brace.

To quantify the strain rate demand on the braces, the time required to increase the tensile stress from zero to the static yield strength before each inelastic excursion was computed from the experimental data. The results of these calculations are summarized, for all the six first floor braces, in Table IV.

The strain rate demand on the braces varies from 10×10^{-3} to 40×10^{-3}/s with a mean value of 22×10^{-3}/s for the three different excitations. The maximum normalized stress observed for each inelastic excursion is also given in Table IV. A good correlation can be observed between the strain rate in the elastic tensile loading portion of the stress–strain curve and the maximum normalized stress reached in the inelastic range of the steel. Figure 6 compares graphically this correlation with the predictions given by equation (1). This empirical equation represents a conservative estimate of the experimental results.

Qualitative examination of impact phenomenon

One phenomenon in earthquake engineering which involves impact loading is the pounding of adjacent buildings during seismic events. Field observations[26–29] and analytical studies[30] have shown that each time

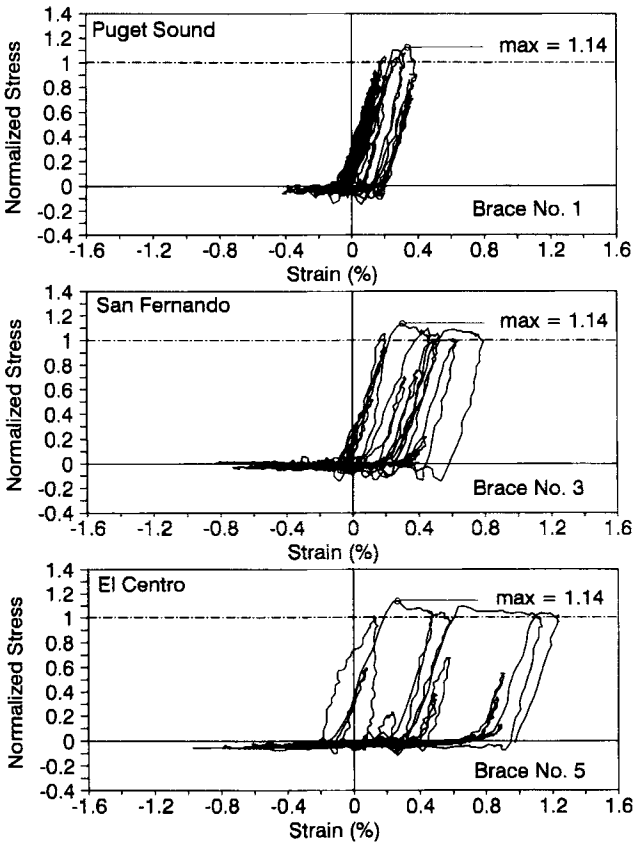

Figure 5. Stress–strain hysteresis loops for first floor brace on east side of frame from shake table tests

an impact occurs, the adjacent structures are subjected to very high amplitude (in excess of 10g), short duration, local accelerations which can induce serious damage to structural and non-structural elements of the buildings.

If the sudden increase in tensile forces in TOCBF causes impact loading, it must, therefore, induce large acceleration pulses at the floor levels where the braces are connected. To investigate if impact phenomena occur in TOCBF, Figure 7 compares the first floor horizontal acceleration time-history with the force time-history recorded in the first floor brace located on the east side of the test frame. This comparison is presented for the first 30 s of each scaled accelerogram considered.

The maximum peak floor accelerations are 0·41, 0·51 and 0·53g for the Puget Sound, San Fernando and El Centro excitations, respectively. These values represent amplifications of the peak base acceleration of only 1·97, 1·52 and 1·30, respectively. These amplifications are one order of magnitude lower than the ones typically observed for seismic pounding. These experimental results indicate that structural and non-structural elements of a TOCBF would not suffer significant additional damage from impact forces during the increase in tensile forces in the braces.

Figure 8 presents, for each earthquake excitation, details of the measured brace force and first floor acceleration around a particular peak force. The floor acceleration increases gradually as the brace force increases in the elastic range. The yield strength of the braces, however, limits the transfer of elastic energy from the moving floor masses to the braces. As the yield plateau in the brace is reached, the acceleration remains constant. No sharp peak in the acceleration time-history is present as it would be the case if a strong impact had occurred.

Table IV. Strain rate demand and maximum normalized stress in first floor braces

Excitation	Brace no.	Inelastic excursion no.	Strain rate $\dot{\varepsilon}$ (10^{-3}/s)	Maximum normalized stress
Puget Sound	1 (East)	1	18	1·07
		2	18	1·06
		3	23	1·06
		4	30	1·14
	2 (West)	1	20	1·01
San Fernando	3 (East)	1	20	1·06
		2	22	1·14
		3	18	1·10
		4	24	1·09
	4 (West)	1	26	1·10
		2	29	1·11
		3	17	1·10
		4	23	1·10
El Centro	5 (East)	1	10	1·01
		2	40	1·14
		3	17	1·05
		4	35	1·10
		5	20	1·04
	6 (West)	No significant inelastic excursion		
Mean strain rate for all inelastic excursions			22	

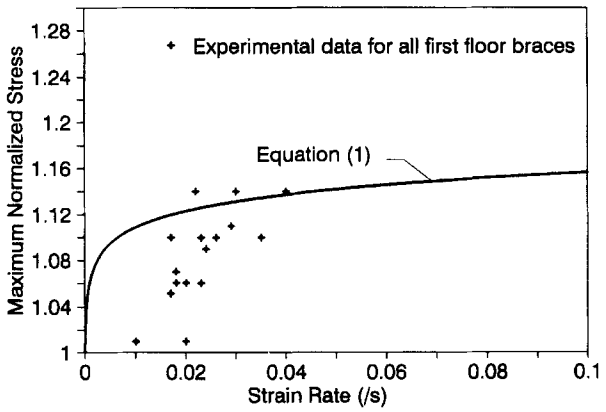

Figure 6. Influence of strain rate on maximum normalized stress in first floor braces

QUASI-STATIC TESTS

Objective and procedure

To visualize clearly the combined effect of strain rate and impact on the seismic response of TOCBF, quasi-static tests were carried out on complete bracing systems under the same inter-storey drift sequence as measured during the seismic shake table tests. For this purpose, the test frame was modified to prevent its first floor from moving horizontally. The first floor concrete block was linked to a rigid reaction frame

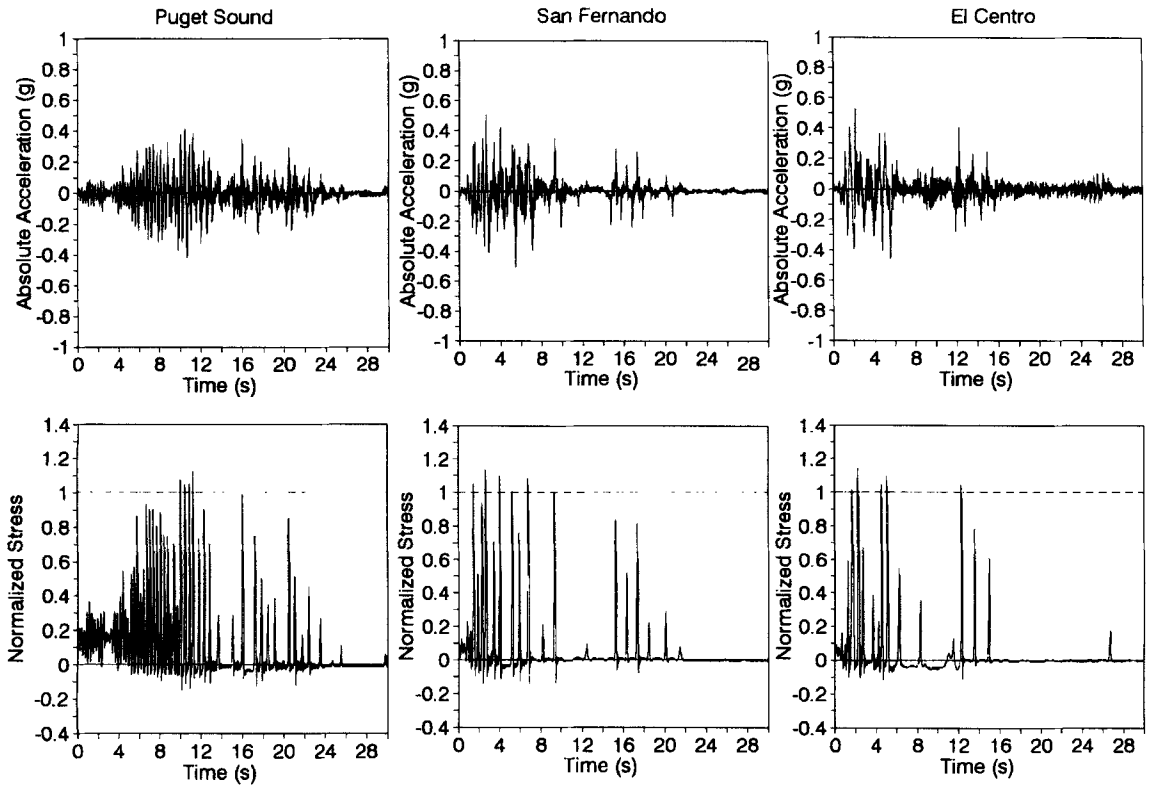

Figure 7. Measured first floor absolute acceleration and first floor east brace force time-histories

located on the strong floor of the laboratory, beside the shake table. For each earthquake excitation, the shake table was controlled by a displacement signal corresponding to the first floor inter-storey drift time-history recorded during the seismic tests. This inter-storey drift signal was played out 400 times slower than recorded to maintain an average strain rate in the first floor braces of 50×10^{-6}/s. This value corresponds to the quasi-static strain rate reference in equation (1). Again, the force time-histories measured in the first floor braces were normalized to the quasi-static yield strength of the steel.

Results

Figure 9 shows, for the El Centro inter-storey drift sequence, the hysteresis loops measured on the first floor brace located on the east side of the frame. Similar results were obtained for the other braces and earthquake excitations. By comparing Figure 9 with the corresponding El Centro hysteresis loops shown in Figure 5, the dynamic effect on a bracing member of TOCBF becomes clear. Under quasi-static conditions, the brace yields at its quasi-static yield strength and does not exhibit any force amplification. Under dynamic conditions, however, the yield strength of steel increases causing an increase in tensile forces in the bracing member.

DYNAMIC TESTS ON STEEL BAR SPECIMENS

Objective and procedure

Monotonic dynamic tensile tests were conducted on steel bars taken from the first floor bracing members used for the shake table investigation. These tests were performed at a prescribed strain rate of 22×10^{-3}/s

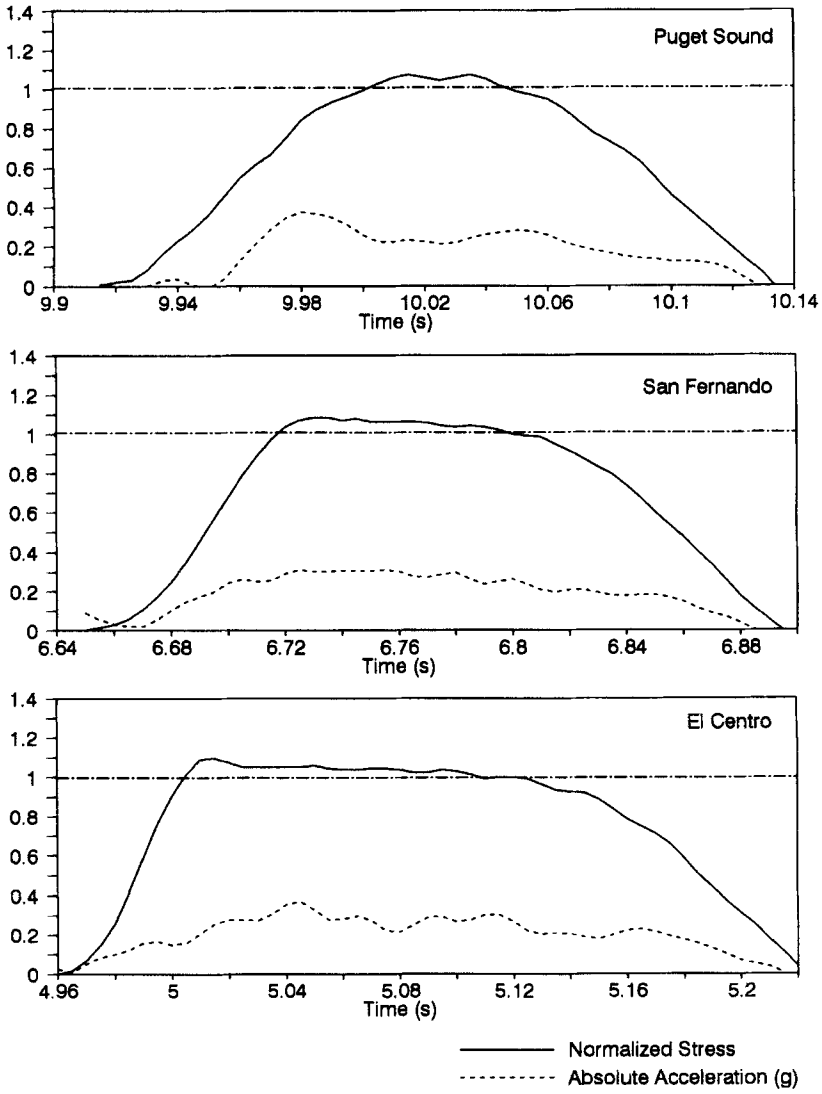

Figure 8. Peak details of measured first floor absolute acceleration and first floor east brace force

corresponding to the mean strain rate demand on the braces during the seismic tests (see Table IV). The specimens, 150 mm long, were tested on a hydraulic servo-controlled testing system. The system was programmed to impose a uniform strain rate to the specimens.

Results

The results of the dynamic tensile tests are shown in Table V. The ratios of dynamic to static yield and tensile strengths are also given in the table. The increase in yield strength due to the strain rate effect is very similar to the maximum normalized stress recorded in the braces during the shake table study. This result confirms that the strain rate effect is the main contributor to the increase in tensile forces in braces of TOCBF. The mean value of 1·12 correlates very well with the prediction of 1·13 given by equation (1) for a strain rate of 22×10^{-3}/s, which indicates that equation (1) is adequate to predict the dynamic yield strength of braces in TOCBF under seismic excitation.

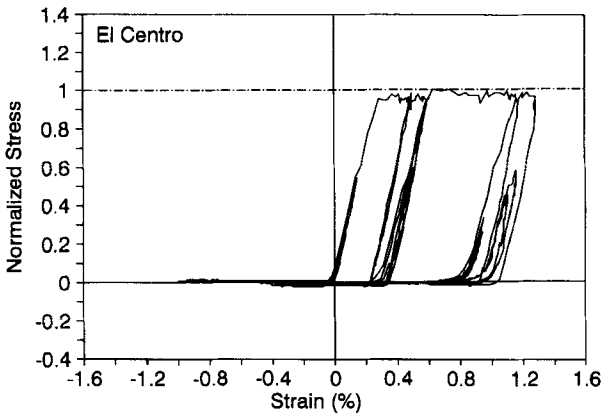

Figure 9. Stress–strain hysteresis loops for first floor brace on east side of frame from quasi-static tests on shake table, El Centro interstorey drift input

Table V. Dynamic* yield and tensile strengths of first floor braces

Brace no.	Yield strength F_{yd} (MPa)	$F_{yd}/F_{ys}^{\dagger}$	Tensile strength F_{ud} (MPa)	$F_{ud}/F_{us}^{\dagger}$
1	356	1·14	490	1·03
2	340	1·09	484	1·02
3	356	1·09	489	1·03
4	359	1·14	481	1·04
5	352	1·12	491	1·07
6	361	1·13	495	1·06
Mean	354	1·12	488	1·04

* Tests performed under a constant strain rate of 22×10^{-3}/s
† Static yield and tensile strength (F_{ys} and F_{us}) taken from Table I

Table V indicates also that the tensile strength of the steel is not as much affected as its yield strength under similar seismic strain rate conditions. The mean tensile strength amplification is only 4 per cent with a maximum of 7 per cent across the six specimens tested. This result is in agreement with previous findings[16–21] and is important for design purposes as discussed later in this paper.

The experimental results presented herein clearly show that the strain rate effect can reconciliate almost completely the sudden increase in tensile forces in TOCBF, leaving no significant contribution from a pure impact phenomenon.

ESTIMATION OF DYNAMIC AMPLIFICATION FACTOR FOR BRACE FORCES

The experimental results reported above indicate clearly that the strain rate effect is directly responsible for the increase in tensile forces in braces of TOCBF. This force increase can be well predicted by equation (1). Therefore, for design purposes, a dynamic force amplification factor could be applied to the brace forces if the maximum strain rate demand in the braces could be approximated for the design earthquake. It is proposed to use a combination of response spectrum and substitute structure techniques to estimate this strain rate demand in the braces.

By definition, the strain rate demand in a bracing element located in the ith storey of a TOCBF, $\dot{\varepsilon}_i$, is equal to the rate of elongation of the element, $\dot{\delta}_i$, divided by its length L_i.

$$\dot{\varepsilon}_i = \frac{\dot{\delta}_i}{L_i} \tag{5}$$

Assuming a predominant shear mode of deformation for low-rise braced frames, the rate of elongation of the bracing element is directly proportional to the rate of inter-storey drift, $\dot{\Delta}_i$, for the storey i hosting the bracing element under consideration.

$$\dot{\delta}_i = C_i \dot{\Delta}_i \tag{6}$$

where C_i is a constant relating the geometries of the bracing element and the floors below and above the ith storey.

Considering that the structure is vibrating in a particular mode of vibration, j, with an effective period of vibration, $T_{j\,\mathrm{eff}}$, and assuming equal elastic and inelastic maximum displacements,[24] the maximum inter-storey drift of the ith storey can be expressed simply by a response spectrum approach.[24]

$$\Delta_i = \alpha_j (A_i^{(j)} - A_{i-1}^{(j)}) S_{\mathrm{D}}^{(j)} \tag{7}$$

where α_j is the participation factor for mode j, $A_i^{(j)}$ and $A_{i-1}^{(j)}$ are the jth mode shape components for floors i and $i-1$, respectively, and $S_{\mathrm{D}}^{(j)}$ is the relative spectral displacement corresponding to the elastic period of vibration and damping ratio in mode, j, T_j and ζ_j. The mode shape components, $A_i^{(j)}$ and $A_{i-1}^{(j)}$, and the modal participation factor, α_j, can be obtained from a free vibration dynamic analysis. Alternatively, assuming that the structure responds in its first mode of vibration ($j = 1$), these parameters can be estimated from the static lateral displacements at floors $i-1$ and i under the code lateral force distribution.

From its initial position, the time necessary for the structure to reach this maximum inter-storey drift (representing one-fourth cycle of vibration) must be equal to one-fourth of the effective period of vibration. Therefore, the average rate of inter-storey drift can be estimated as follows:

$$\dot{\Delta}_i = \frac{4\alpha_j (A_i^{(j)} - A_{i-1}^{(j)}) S_{\mathrm{D}}^{(j)}}{T_{j\,\mathrm{eff}}} \tag{8}$$

The inelastic response of the structure must be reflected by the appropriate value for the effective period of vibration to be used in equation (8). For this purpose, the substitute structure approach[31,32] is considered. This substitute structure approach is a procedure where an inelastic system is modelled as an equivalent elastic system as shown in Figure 10. For a TOCBF vibrating in a particular mode j of vibration, the stiffness, K_j, corresponds to the elastic stiffness of the tensile braces before yielding. The effective stiffness, $k_{j\,\mathrm{eff}}$, is the secant stiffness corresponding to a maximum inelastic displacement characterized by a displacement ductility factor, μ. With these assumptions, the effective period of vibration, $T_{j\,\mathrm{eff}}$, can then be simply related to the elastic period of vibration, T_j.

$$T_{j\mathrm{eff}} = \sqrt{\mu}\, T_j \tag{9}$$

Substituting equations (6), (8) and (9) into equation (5), yields an expression for the average strain rate demand in the braces at a particular storey, i, in the structure.

$$\dot{\varepsilon}_i = \frac{4C_i \alpha_j (A_i^{(j)} - A_{i-1}^{(j)}) S_{\mathrm{D}}^{(j)}}{\sqrt{\mu} T_j L_i} \tag{10}$$

The average strain rate demand can also be written as a function of the pseudo-absolute spectral acceleration, $S_{\mathrm{A}}^{(j)}$.

$$\dot{\varepsilon}_i = \frac{C_i \alpha_j (A_i^{(j)} - A_{i-1}^{(j)}) T_j S_{\mathrm{A}}^{(j)}}{\pi^2 \sqrt{\mu} L_i} \tag{11}$$

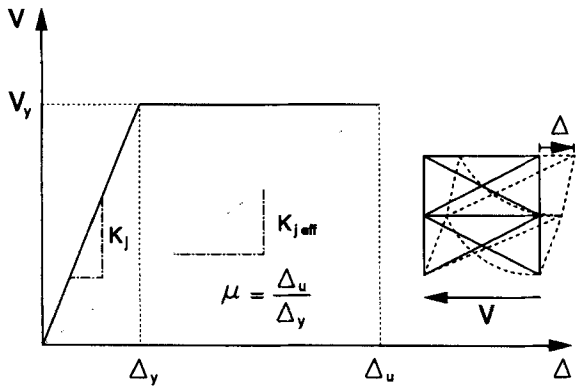

Figure 10. Substitute structure approach for seismic response of a TOCBF

Table VI. Dynamic amplification factor (D_{b1}) for first floor braces of test frame

Excitation	C_1*	α_1	$A_1^{(1)}$	T_1† (s)	$S_A^{(1)}$‡ (m/s²)	μ§	L_1 (m)	$\dot{\varepsilon}_1$ (10^{-3}/s)	D_{b1}
Puget sound					8·7	2·4		64	1·15
San Fernando	0·87	1·27	0·53	0·47	6·0	4·9	2·5	31	1·13
El Centro					13·3	7·7		42	1·14

*cosine of angle of inclination of braces from horizontal
†see Table II
‡see Figure 4
§see Figure 5

Finally, the substitution of equation (11) into equation (1) leads to an expression for the dynamic amplification factor for the braces located in the ith storey, D_{bi}, of a TOCBF vibrating in a particular mode j.

$$D_{bi} = 1 + 0{\cdot}0473 \log\left[\frac{C_i \alpha_j (A_i^{(j)} - A_{i-1}^{(j)}) T_j S_A^{(j)}}{50 \times 10^{-6} \pi^2 \sqrt{\mu L_i}}\right] \tag{12}$$

Table VI presents the application of equation (12) to the first floor braces of the TOCBF models tested on the shake table. The calculations were performed for the first elastic mode of vibration of the structure ($j = 1$). The coefficient C_1 is simply equal to the cosine of the inclination angle of the braces from the horizontal. A linear free vibration analysis was performed on the test frame to determine the first modal participation factor, α_1, and the first floor component of the first mode shape, $A_1^{(1)}$. The mode shape component $A_0^{(1)}$ is equal to zero for the first storey. The spectral accelerations in the first mode of vibration, $S_{A1}^{(1)}$, were read directly from Figure 4. The ductility ratios, μ, were obtained from Figure 4.

The results of the calculations shown in Table VI agree well with the experimental data shown in Table IV. The maximum strain rate demands are reasonably well predicted by this simple approach. The resulting force amplification factors are, on the other hand, virtually identical as the maximum normalized stress measured in the first floor braces during the seismic tests (see Figure 5). Equation (12) is, therefore, adequate for estimating, at the design stage, the increase in tensile forces in braces of TOCBF due to strain rate effect.

The logarithmic function in equation (1) makes the force amplification factor relatively insensitive to the strain rate. The maximum strain rates that can be generated by seismic excitation is conservatively estimated as 10^{-1}/s. According to equation (1) and as shown in Figure 6, the maximum value for the dynamic

amplification factor of a bracing member would be equal to 1·15. This conservative estimate could be used for code design purposes.

DYNAMIC AMPLIFICATION FACTOR FOR ADJACENT ELEMENTS

General

From the experimental results generated in this investigation, it has become clear that the increase in tensile forces in braces of TOCBF is mainly caused by the increase of the yield strength of the steel under high strain rate demand. Adjacent elements in the lateral load resisting system will experience similar strain rate demands as in the braces. The resistance of these elements must then be also influenced by the strain rate. Therefore, the dynamic amplification factor for the design of these other elements, D_e, must depend on their failure criteria. Three different cases must be distinguished, depending upon the critical failure mode considered for their design:

(1) ductile mode of failure;
(2) brittle mode of failure;
(3) buckling mode of failure.

Ductile mode of failure

If failure of an adjacent element is ductile, its associated resistance is based on the yield strength of steel. The yield strength of this ductile member will also increase by a similar amount as in the bracing elements. Therefore, a dynamic amplification factor equal to unity should be applied for the design of this ductile element.

$$D_e = 1{\cdot}0 \tag{13}$$

Brittle failure mode

If failure of an adjacent element is brittle, its design is based on the tensile strength of steel, which will be affected differently by the strain rate demand on the adjacent bracing elements. As shown in Table V, the tensile strength of steel increases by a smaller amount than the yield strength in the bracing elements. Therefore, the dynamic amplification factor to be used for the design of this brittle element should be equal to the dynamic amplification factor for the adjacent braces, D_b, divided by the increase of its tensile strength under the same strain rate demand (F_{ud}/F_{us}).

$$D_e = \frac{D_b}{D_u} \tag{14}$$

where

$$D_u = \frac{F_{ud}}{F_{us}} \tag{15}$$

Currently, no relation is available to relate the increase of tensile strength of steel to the strain rate demand. The experimental data generated in this investigation indicate that the increase in tensile strength of steel could be taken as 1·05 for a seismic strain rate demand. This factor, however, can conservatively be taken equal to 1·0 for design purposes.

Buckling mode of failure

If failure of an adjacent element would occur by elastic buckling, its resistance will not be affected by the strain rate demand on the adjacent bracing elements. If failure of an adjacent element occurs by inelastic buckling, its resistance will be affected to some extent by the strain rate demand on the adjacent bracing elements. The dynamic amplification factor to be used in this case would lie between a value of unity, for an

inelastic ductile failure mode, and D_b, for an elastic buckling mode of failure. The amount of inelastic behaviour can be evaluated from the slenderness factor λ used by steel codes to evaluate the compressive strength of columns.[14,15]

$$\lambda = \frac{KL}{r}\sqrt{\frac{F_{ys}}{\pi^2 E}} \tag{16}$$

where KL/r is the slenderness ratio of the element under consideration and E is the elastic modulus.

If $\lambda = 0$, the member can reach its yield strength and a force amplification factor of unity should be applied for its design. If $\lambda = 1{\cdot}5$, failure of the member is characterized by a nearly elastic buckling mode[33] for which the full value of D_b should be applied for its design. For intermediate values of λ, the force amplification factor to be used could be equal to D_b divided by an inelastic modification factor such as:

$$D_e = \frac{D_b}{0{\cdot}67(1 - D_b)\lambda + D_b} \leqslant D_b \tag{17}$$

Equation (17) simplifies the effect of residual stresses on the compressive strength and may need to be refined for certain types of elements.

CONCLUSION

The results of half-scale, two-storey TOCBF models have provided an opportunity to shed some light on the increase in tensile forces in the bracing elements of these steel structures. Based on the experimental results obtained, the following conclusions can be drawn:

(1) The sudden increase in tensile forces in the braces of TOCBF, as they become suddenly taut, are limited by the yield strength of the steel. This hysteretic effect limits the transfer of elastic energy from the moving floor masses to the braces and, thereby, attenuates the impact forces on the connections and other structural elements. The increase in tensile forces in the braces of TOCBF is, therefore, mainly caused by a yield strength increase of the steel under a high strain rate demand. This strain rate effect may also occur in other lateral load resisting systems such as frames with tension–compression acting braces.

(2) A simple equation, based on a combination of response spectrum and substitute structure techniques, has been proposed to estimate this increase in brace forces at the design stage. The predictions of this proposed equation correlates well with the shake table results obtained herein. Alternatively, a conservative dynamic amplification factor for the braces of 1·15 could be used for preliminary code design applications.

(3) The resistance of adjacent elements in the lateral load resisting system is also influenced by the strain rate. The dynamic amplification factor for the design of these elements must depend on their failure criteria.

ACKNOWLEDGEMENTS

The authors acknowledge the assistance of the Natural Science and Engineering Research Council of Canada (NSERC) and the Fonds pour la Formation de Chercheurs et l'Aide à la Recherche (FCAR) of Quebec which provided research grants in support of this project. The assistance of the Group CANAM MANAC of Montreal, which supplied the testing material, is also gratefully acknowledged. The authors wish to express their appreciation to Ms. Julie Gagné, research assistant, for her contribution to the experimental part of the project. The technical staff of the Structures Laboratory at Ecole Polytechnique is sincerely acknowledged for its invaluable assistance.

REFERENCES

1. E. P. Popov and V. V. Bertero, 'Seismic analysis of some steel building frames', *J. eng. mech. div. ASCE* **106**, 75–93 (1980).
2. X. Tang and S. C. Goel, 'Seismic analysis and design considerations of braced steel structures', *Research report UMCE 87-4*, Department of Civil Engineering, University of Michigan, Ann Arbor, MI, 1987.
3. Y. Takahashi, N. Nakamura, B. Kato and T. Seaki, 'Study on restoring force characterisitics of x-steel braces', *Proc. 10th world conf. on earthquake eng.* Madrid, Spain, A. A. Balkema Publishers, Brookfield, USA. **5**, 2931–2936 (1992).
4. K. Takanashi and K. Ohi, 'Shaking table tests on 3-story braced and unbraced steel frames', *Proc. 8th world conf. on earthquake eng.* (San Francisco, CA), Prentice-Hall Inc., Englewood Cliffs, New Jersey **VI**, 193–200 (1984).
5. L. S. Wijanto, P. J. Moss and A. J. Carr, 'The seismic behaviour of cross-braced steel frames', *Earthquake eng. struct., dyn.* **21**, 319–340 (1992).
6. G. Zingone and M. Papia, 'Energy dissipation capacity of stiffened steel systems under high intensity earthquake', *Proc. 8th world conf. on earthquake eng.*, San Francisco, CA, **IV**, 499–506 (1984).
7. S. C. Goel and A. Astaneh-Asl, 'Cyclic behavior of double angle bracing members with welded connections', *Proc. 8th world conf. on earthquake eng.*, San Francisco, CA, **VI**, 241–248 (1984).
8. F. Peroti and G. P. Scarlassara, 'Concentrically braced steel frames under seismic actions: non-linear behaviour and design coefficients', *Earthquake eng. struct. dyn.* **20**, 409–427 (1992).
9. A. Jain, S. Goel and R. D. Hanson, 'Hysteretic cycles of axially loaded members', *J. struct. div. ASCE* **106**, 1777–1795 (1980).
10. G. R. Black, W. A. Wenger and E. P. Popov, 'Inelastic buckling of steel struts under cyclic load reversal', *EERC Report 80-40*, University of California, Berkeley, CA, 1980.
11. R. Tremblay, M.-H. Archambault and A. Filiatrault, 'Seismic behavior of ductile concentrically steel x-bracings', *Proc. 7th Canadian conf. on earthquake eng.*, Montreal, Canada, 549–556 (1995).
12. FEMA, 'NEHRP recommended provisions for seismic regulations for new buildings Part 1–provisions', Federal Emergency Management Agency, *FEMA 222A*, Building Seismic Safety Council, Washington, DC (1994).
13. SEAOC, 'Recommended lateral force requirements and commentary', Seismology Committee, Structural Engineers Association of California, Sacramento, CA (1990).
14. AISC, 'Seismic provisions for structural steel buildings', American Institute of Steel Construction (1992).
15. CSA, 'Limit state design of steel structures', National Standard of Canada, *CAN/CSA-S16. 1-94*, Canadian Standards Association, Rexdale, Ontario, 1994.
16. M. Wakabayashi, T. Nakamura, S. Iwai and Y. Hayashi, 'Effects of strain rate on the behavior of structural members', *Proc. 8th world conf. on earthquake eng.*, San Francisco, CA, **IV**, 491–498 (1984).
17. K. Udagavva, K. Takanashi and B. Kato, 'Effects of displacement rates on the behavior of steel beams and composite beams', *Proc. 8th world conf. on earthquake eng.*, San Francisco, CA, **VI**, 177–184 (1984).
18. K. Kaneta, I. Kohzu and K. Fujimura, 'On the strength and ductility of steel structural joints subjected to high speed monotonic tensile loading', *Proc. 8th European conf. on earthquake eng.*, Lisbon, Portugal, **4**, 7.2/17–7.2/24 (1986).
19. Y. Nagataki, Y. Kitagawa, M. Midorikawa and T. Kashima, 'Dynamic response analysis with effects of strain rate and stress relaxation', *Proc. 9th world conf. on earthquake eng.*, Tokyo-Kyoto, Japan, **IV**, 693–698 (1988).
20. K. Suita, K. Kaneta and I. Khozu, 'The effect of strain rate in steel structural joints due to high speed cyclic loadings', *Proc. 10th world conf. on earthquake eng.*, Tokyo-Kyoto, Japan, 2863–2866 (1992).
21. K. Sugiura, K. C. Chang and G. C. Lee, 'Strain rate and its history effect on the inelastic material behavior of structural steel under multiaxial stress condition', *Proc. 9th world conf. on earthquake eng.*, Tokyo-Kyoto, Japan, **IV**, 103–108 (1988).
22. A. Filiatrault, R. Tremblay, B. K. Thoen and J. Rood, 'A second generation earthquake simulation system in Canada: description and performance', *Proc. 11th world conf. on earthquake eng.*, Acapulco, Mexico, Edited by Sociedad Mexicana de Ingeniería sismica, A. C., Permagon, (1996). Paper No. 1204, on CD-ROM.
23. EDI, 'U2 and V2 Manual', Experimental Dynamic Investigations Ltd., Vancouver, Canada, 1993.
24. R. W. Clough and J. Penzien, *Dynamics of Structures*, 2nd edn, McGraw-Hill, New York, 1993.
25. NRCC, 'National Building Code of Canada', Associate Committee on the National Building Code, National Research Council of Canada, Ottawa, Ontario, 1995.
26. G. V. Berg and J. H. Degenkolb, 'Engineering lessons from the Managua earthquake', *American and Steel Institute Report*, 1973.
27. E. Rosenblueth and R. Meli, 'The 1985 earthquake: causes and effects in Mexico City', Concrete International, American Concrete Institute **8**(5), 23–24 (1986).
28. V. V. Bertero, 'Observations of structural pounding' in *Proc. ASCE int. conf. on the 1985 Mexico city earthquake*, 1986.
29. K. Kasai and B. F. Maison, 'Observation of structural pounding damage from the 1989 Loma Prieta earthquake', *Proc. 6th Canadian conf. on earthquake eng.*, Toronto, 735–742 (1991).
30. K. Kasai, V. Jeng and B. F. Maison, 'The significant effects of pounding-induced accelerations on building appurtenances', Applied Technology Council, ATC-29, *Proc. seminar and workshop on seismic design and performance of equipment and nonstructural elements in buildings and industrial structures*, Irvine, CA, 1990.
31. P. Gulkan and M. Sozen, 'Inelastic response of reinforced concrete structures to earthquake motions', *ACI J.* **71**, 604–610 (1974).
32. A. Shibata and M. Sozen, 'Substitute structure method for seismic design in R/C', *J. struct. div. ASCE* **102**, 1–18 (1976).
33. C. G. Salmon and J. E. Johnson, 'Steel structures—design and behavior', Harper & ROW, New York, 1990.